Zeitschrift für Geomorphologie, Vol. 60/3 (2016), 195-208
Published online May 2016; published in print September 2016

Article

ALOS-derived glacier and rock glacier inventory of the Volcán Domuyo region (~36° S), southernmost Central Andes, Argentina

Daniel Falaschi[1]*, Mariano Masiokas[1], Takeo Tadono[2], Fleur Couvreux[3]

[1] Instituto Argentino de Nivología, Glaciología y Ciencias Ambientales (IANIGLA). CCT-CONICET Mendoza C.C. 330 – (5500) Mendoza, Argentina.
[2] Earth Observation Research Center (EORC), Japan Aerospace Exploration Agency (JAXA), 2-1-1, Sengen, Tsukuba, Ibaraki 305–8505, Japan.
E-mail: tadono.takeo@jaxa.jp
[3] Météo-France, CNRM/GMME/MOANA, 42 Av. Coriolis (31057) Toulouse Cedex 1, France.
E-mail: fleur.couvreux@meteo.fr
* dfalaschi@mendoza-conicet.gov.ar

With 8 figures and 1 table

Abstract: In this study we use optical ALOS AVNIR-2 and PRISM satellite images to map and inventory glaciers as well as active, inactive and fossil rock glaciers in the Volcán Domuyo region (36°16' S–36°54' S), located in the northwestern tip of the Neuquén Province in Argentina. The area is termed "Transition Cordillera" since it lies between the southernmost reaches of the Central Andes and the Patagonian Andes. We inventoried a total of 106 glaciers, covering an area of ~25.4 km^2, and 173 intact rock glaciers (~11.3 km^2) in the year 2009. Using a 1990 Landsat scene from this area, we estimated a retreat rate of 26% reduction (~1.4% per year) of the glacier covered area between 1990 and 2009. The minimum elevation of the front talus of active rock glaciers indicates that the lower limit of discontinuous mountain permafrost in the region is located around 2800 m a.s.l. The results here provide new information about the current extent and recent behavior of glaciers and the spatial distribution of mountain permafrost in this poorly known region of the southern Andes. The lack of complete, long climate records in the area precludes detailed analyses of the recent response of glaciers to climate variability. However, regional warming trends and a recent reduction in winter precipitation may have contributed to the observed recent glacier wastage in the Domuyo region.

Keywords: glacier inventory, rock glacier inventory, glacier fluctuations, mountain permafrost, Volcán Domuyo, Central Andes, Argentina

1. Introduction

Glaciers in the Andes of Argentina and Chile between 36°S and 45°S are mostly associated with large volcanic edifices (Rivera et al. 2012, Trombotto Liaudat et al. 2014), Volcán Domuyo (36–37° S) being one of the most prominent cases.

In Argentina, a federal initiative aiming to inventory and monitor all glaciers and rock glaciers in the country has been running since 2010. Under this initiative, glaciological research has not only been concentrated in the historical targets – the large outlet glaciers on the eastern side of the Southern Patagonian Icefields (e.g. Rivera et al. 2012, Willis et al. 2012, De Angelis 2014), but has recently shifted to other, less studied glaciated areas in the Andes (e.g., Leclerq et al. 2012, Falaschi et al. 2013, Masiokas et al. 2015). These smaller glaciers may also contribute to improve our understanding of the climate-cryosphere interactions in different Andean environments.

Active rock glaciers, which are the visible expression of steady-sate creep of ice-saturated mountain permafrost (Haeberli 1985), also have their own hydrological relevance in water-stressed regions (Brenning 2005). These tongue- or lobate-shaped bodies of frozen unconsolidated material have been studied and described in detail in the

DOI: 10.1127/zfg/2016/0319

Central Andes of Chile and Argentina around 30–33 °S (e.g. Perucca & Angillieri 2008, Esper Angillieri 2009, Tombotto & Borzotta 2009, Bodin et al. 2010, Brenning & Azócar 2010), but have received little attention further south in the Andes.

The main goal of this study was the completion of a first glacier and rock glacier inventories for the Volcán Domuyo area, providing important basic information (such as location, extent, altitudinal range). We were also interested in assessing glacier area changes between 1990 and 2009, and discussing possible climatic trends that may help explain the observed glacier changes.

2. Study area and previous studies

The Volcán Domuyo (36°38' S, 70°25' W, 4706 m a.s.l.) is an eroded stratovolcano located in the Argentinean Neuquén Province, ca. 50 km east of the main Andean axis. The study region is characterized by high relief, dominated by the volcano itself but also including the Cordillera del Viento to the south and Sierra de Cochico subsidiary ranges to the northwest (Fig. 1), both of which slightly exceed 3000 m a.s.l. The Domuyo ice masses feed the Neuquén River, the fundamental contributor to the development of the Río Negro valley flourishing agriculture area, and also contribute with freshwater to one of Argentina's most important hydropower systems. Hence, these ice masses constitute an important reserve and source of meltwater for several local socio-economic activities.

Previous studies in the area have concentrated in the geology and stratigraphy of the volcanic and sedimentary rocks (Llambías et al. 1978, 1978b). The basement in the region is composed by the Permo-Triassic volcanic rocks of the Choiyoi Group (Rolleri & Criado Roque 1970), which is covered by the Mesozoic sedimentary formations of the Neuquén Basin, including marine (Mendoza Group, Digregorio & Uliana 1980) and continental (Neuquén Group, Digregorio 1972) deposits. The Cenozoic igneous rocks comprehend andesites and rhyolites of Oligocene to lower Pleistocene age; Pleistocene to Holocene are represented by trachyte and basalt flows, glacial and periglacial sediments, and modern piedmont deposits filling valley floors.

From a historical point of view, Groeber (1946) was probably the first to reach the foot of the glaciers at the base of the eastern face of the Volcán Domuyo, depicting in a sketch the position of these glaciers at that time. Mercer (1967), mentioned "small glaciers in the summit areas of the volcano" in his southamerican glacier Atlas. This volcano is enclosed in a region with drier conditions than the Patagonian Andes, although the amount of available moisture in this area is higher than in the Central Andes further north. The Andean glaciers between 31° S and 38° S receive precipitation driven by the mid-latitude westerly flow that reaches the area during the winter season (Sagredo & Lowell 2012). Nogami (1972) stated that they are subjected to temperature variations between –5.3 °C in winter and 5.5 °C during the summer, the snowline decreasing from 5000 m a.s.l. in the north of this latitudinal belt to ca. 2800 m a.s.l. at around 38° S.

With regards to rock glaciers, very little previous information is available. Inactive landforms were vaguely mentioned in the region by González Díaz & Folguera (2005, 2011).

3. Data sets and method

3.1. Glacier and rock glacier mapping

In this study we perform a glacier and rock glacier inventory (Fig. 1) using scenes from the ALOS (Advanced Land Observing Satellite) datasets, obtained from the Japan Aerospace Exploration Agency (JAXA). The glacier inventory was based on an ALOS AVNIR2 orthorectified 10 m spatial resolution satellite image dating from April 2009, which coincides with the very end of the ablation (dry) period. Compared to other optical sensors such as Landsat or ASTER, which have been broadly used for the compilation of glacier inventories worldwide, the AVNIR2 sensor offers a higher pixel resolution but lacks a short wave infrared (SWIR) spectral band. This, in turn, precludes the semi-automatic identification of glacier ice by means of band ratio thresholding (Racoviteanu et al. 2009). Thus, the mapping of ice masses in this study was accomplished using a supervised classification of a false color RGB 321 composite in the open source SPRING GIS software (www.dpi.inpe.br). Due to the large extension of debris-covered ice, which has similar spectral properties with respect to the surrounding ice-free bedrock and glacier forefields (and thus cannot be identified automatically), a fair amount of manual corrections were applied to obtain the final outlines using the open source KOSMO GIS software (www.opengis.es). Following the Global Land Ice Measurement from Space (GLIMS) initiative guidelines, the minimum glacier area was fixed at 0.01 km^2.

Glacier areal shrinkage for the 1990–2009 period was calculated using a 30 m resolution, March 1990 Landsat TM scene, obtained from the online Data Pool at the NASA Land Processes Distributed Active Archive Center (LP DAAC), USGS/Earth Resources Observation and Science (EROS) Center, Sioux Falls, South Dakota (http://lpdaac.usgs.gov/get_data). In this case the band ratio method (TM3/TM5) was used to identify bare ice, with a final threshold of DN>2, and additional manual

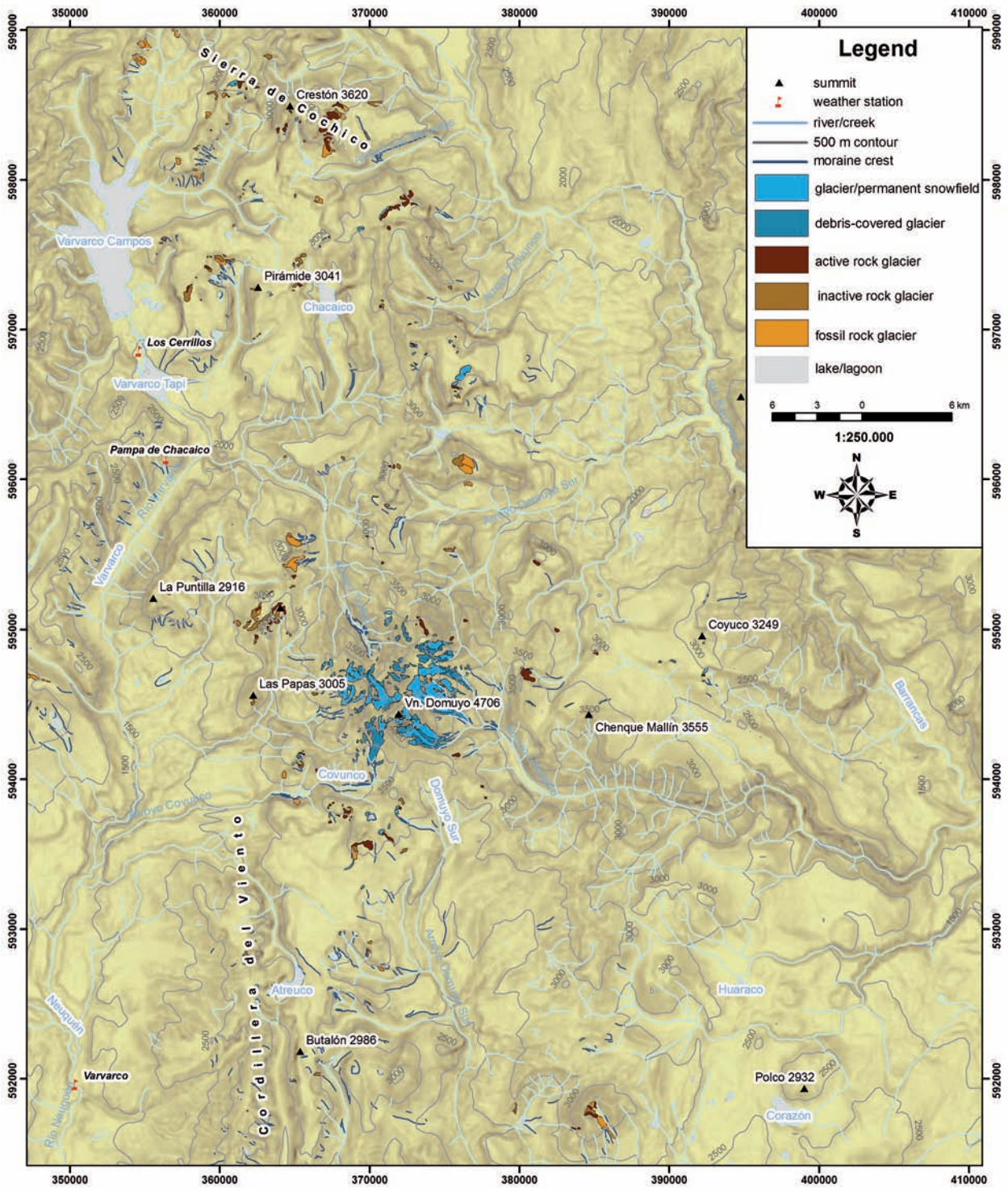

Fig. 1. Study site location and inventory maps.

digitizing as described above. Both the ALOS and Landsat images were acquired at the very end of the ablation period and present superb conditions for glacier mapping (i.e. no seasonal snow and no clouds).

Because rock glaciers have spectral properties similar to the surrounding terrain and headwalls, the limits of these landforms are often difficult to define. This highlights the importance of using high-resolution optical satellite images for rock glacier mapping. In this study, the rock glacier inventory was performed using a 2.5 m resolution ALOS PRISM mosaic, acquired on the same date as the AVNIR2 scene. Rock glaciers were classified as active, intact or fossil landforms (Barsch 1996) based on geomorphologic criteria visible in the high resolution PRISM images. Fossil rock glaciers result from continuous thaw followed by permafrost degradation (Ikeda & Matsuoka 2002), and they may be disconnected from the active talus shed. Here, fossil landforms were identified as those usually having gentle dipping front slope (usually <35°), a subdued surface topography with mostly poorly preserved furrows and ridges, large block accumulations at the talus feet, and the growth of variable amounts of vegetation on the landform's frontal and lateral slopes (Haeberli 1985, Brenning 2005, Kääb 2007).

Further morphological indicators were used to infer rock glacier activity and classify them as active and inactive features. Above all, steep front talus (usually >45°), the good preservation of the surface furrows and ridges topography, and the lack of large boulders accumulation at the talus foot were considered indicative of active rock glaciers. Additionally, the presence of freshly exposed, fine debris at the top of the rock glacier front pinpoints an angle greater than the angle of repose of the loose material, which was also used as indicative of an active advancing front.

An ALOS PRISM stereopair was used to build a 10 m resolution digital surface model (DSM), by means of the DSM and Ortho-image Generation Software, specially developed for PRISM data by the Japan Aerospace Exploration Agency (JAXA). No in situ Ground Control Points (GCP) measurements were used in the process, but Takaku & Tadono (2009) have previously indicated that the horizontal accuracy of a relative ALOS PRISM DSM is below 6 m and the vertical accuracy lies between 2 and 18 m without the benefit of GCPs. The DSM was used to automatically delineate hydrological basins and ice divides, though manual corrections of outlines were sometimes necessary due to minor artifacts on the DSM. Additionally, the DSM grid was used to extract altitudinal data, derive glacier and rock glacier morphometric parameters (minimum and maximum elevation, mean slope, aspect), and to obtain glacier hypsometries. Glacier average thickness along the central flow line h_f (m) was calculated using the empirical relation between glacier elevation range ΔH and the basal shear stress τ presented by Haeberli & Hoelzle (1995),

$$h_f = \frac{\tau}{f \cdot \rho \cdot g \cdot \sin\alpha} \qquad (1)$$

where τ = mean basal shear stress along the central flow line (bar), f = shape factor (0.8 for all glaciers); ρ = density of ice (900 kgm^{-3}; Salzmann et al. 2013); g = gravitational acceleration (9.8 ms^{-2}) and α = average surface slope of the glacier retrieved from the DSM. This way, the glacier outlines and corresponding thicknesses provide a rough estimation of total glacier volume for the region.

3.2. Assessment of mapping error

Various types of error may be introduced when mapping glacier outlines and estimating glacier areal changes from satellite images. The origin, magnitude and ease of quantification of each of them are discussed in Paul & Andreassen (2009). Precisely because of the difficulties found when estimating mapping errors, previously published glacier inventories have rarely reported these uncertainties. For glaciers composed of clean ice in their entirety, we followed the approach of Paul et al. (2013), who found that the digitizing accuracy on medium resolution satellite images is comparable to the pixel size, and calculated the rough precision by buffering the area by one pixel and calculating the relative change in glacier size.

Errors derived from overestimating glacier size due to seasonal snow were neglected, since a) the close examination of both the ALOS and Landsat images reveal little if any seasonal snow and b) the scenes were acquired right at the end of the ablation period of two considerably dry years in the Central Andes (Masiokas et al. 2012).

The mapping error when digitizing rock glaciers is much more difficult to ascertain. The borderline with their respective contributing areas or the surrounding terrain, which can contain sediment in transit, is often hard to define. Consequently, and in addition to spatial resolution, rock glaciers outlines fully digitized by means of visual interpretation and manual digitizing will be entirely subject to the analyst's expertise and subjectivity, and their accuracy will be difficult to ascertain without exhaustive ground-truth data. Incidentally, Paul et al. (2003) proposed that 10 m resolution optical images were necessary for validation of permafrost distribution maps. To make matters worse, and in contrast with glaciers, no automatic rock glacier mapping algorithms exist that can be used as reference values to be compared against the manually derived outlines.

Here we produced a digitalization round, inspired and similar to the experiments by Paul et al. (2013), to estimate the mapping variability as a function of image resolution. In such an experiment, the outlines of ten rock glaciers produced by ten different analysts derived from different spatial resolution optical images are compared. These consisted in the PRISM (2.5 m) and AVNIR2 (10 m) ALOS images, and an Advanced Spaceborne Thermal Emission and Reflection Radiometer (ASTER) 15 m scene. This way, the mean values of the multiple digitalizations on the high-resolution imagery (which in our case was the PRISM scene) are used as the rock glacier area reference. The multiple digitalization of the low resolution data provide not only a measure of the precision of the analysts mapping, but also a mean value for comparison with the high resolution derived reference as well. Finally, area buffers of 1, 2 and 3 pixels applied to the reference outlines stemming from the ALOS PRISM mapping are compared against the variability of the digitalization rounds in different resolutions.

3.3. Mountain Permafrost Limit, glacier Equilibrium Line Altitude and climate records

The Mountain Permafrost Limit (MPL hereafter), that is, the lowermost elevation of discontinuous mountain permafrost, was estimated from the occurrence of the lowermost active rock glacier fronts (Brenning 2005). This elevation is also used to calculate rock glacier density as the ratio between the area covered by active rock glaciers and the area above the MPL.

On the other hand, glacier Equilibrium Line Altitude (ELA) was obtained from Condom et al. (2007), who derived glacier ELAs for the Southamerican Andes based on the gridded temperature and precipitation data from New et al. (2000). Additionally, Mean Annual Air Temperature (MAAT) at glacier ELA was used to infer glacier thermal regimes (englacial temperatures), which in turn is indicative of the regional climate and continentality. Because long, high elevation temperature records near glaciated areas are rare in this region, present-day MAAT (see section 5.1) was calculated from the 1997–2013 temperature records of Pampa de Chacaico weather station (36°28' S – 70°36' W, 2580 m, Fig. 1), with a lapse rate of 0.65 °C/100 m.

One of the longest available temperature records stems from the Varvarco station (36°51' S – 70°40' W, 1190 m, Fig. 1), which is located ca. 30 km south of Volcán Domuyo. This data shows good correlations with gridded ERA Interim reanalysis temperatures at the 700 mb geopotential height. This gridded dataset has 0.75° x 0.75° spatial resolution and is available since January 1979 (Dee et al. 2011). The positive association between these independent datasets suggests they are probably reliable and were thus used to assess recent summer temperature variations in this region.

4. Results

4.1. Glacier inventory and area changes

A total of 106 glaciers and perennial snow patches totaling 25.4 km^2 were identified in the Domuyo area in April 2009. Figure 2A provides an overview of the glacier area distribution. Small area classes (0.01–0.1 km^2 and 0.1–0.5 km^2 consist mainly of permanent snowfields and glacierets. These smaller units are much more numerous than the larger mountain glaciers (>1 km^2) but represent a much smaller total glaciated area. In fact, 82% of the total ice bodies are smaller than 0.1 km^2, but they merely

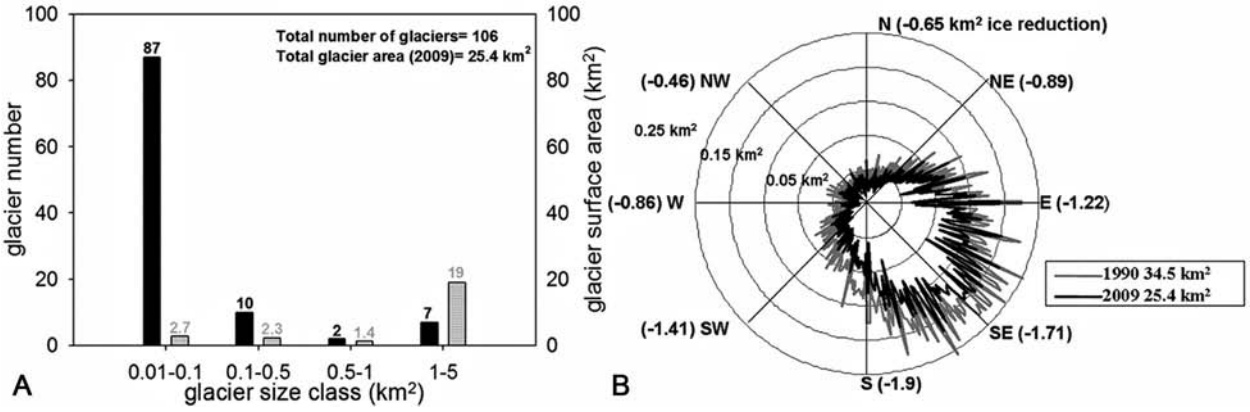

Fig. 2. (A) Bar graph depicting the inverse relation between the number of glaciers (black bars) and the ice-covered area by the respective glacier size classes (grey bars). (B) Orientation of the ice-covered area in the Volcán Domuyo region in 1990 (gray) and 2009 (black). The values in parentheses indicate absolute ice losses in square kilometers for each cardinal sector.

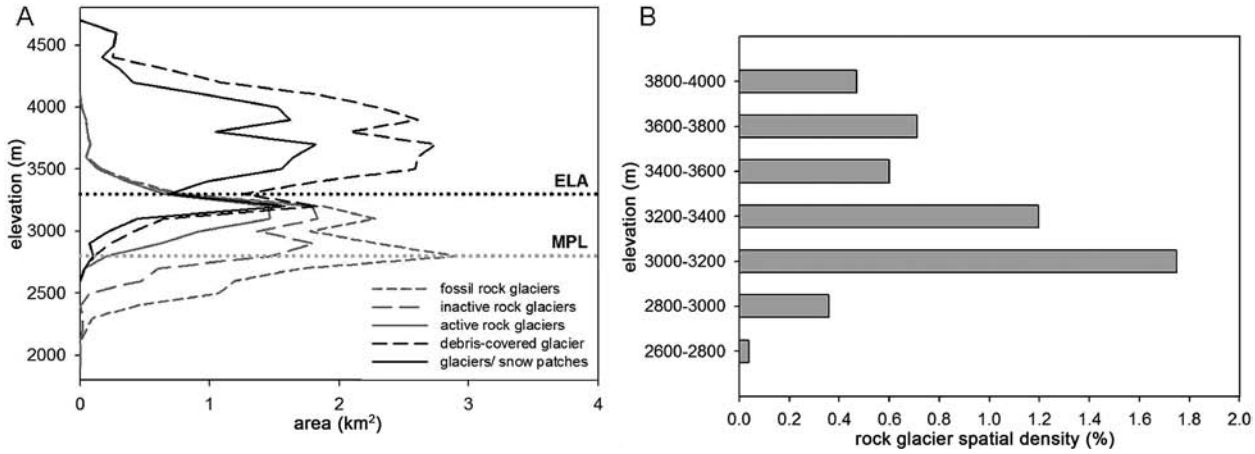

Fig. 3. (A) Altitudinal distribution of the ice-covered area (with the debris-covered and debris-free relative amount) and rock glaciers (active, inactive and fossil). The dotted horizontal lines represent the equilibrium line altitude (ELA, Condom et al. 2007) and the lower limit of mountain permafrost after Cheng & Dramis (1992).

represent ~11% of the total ice covered area. In comparison, glaciers larger than 1 km^2 contribute no more than 6% of the total inventory in number but represent ~75% of the total glacier area. For the 2009 glacier inventory, the total glacier volume was estimated in 1.1 km^3 by means of the parameterization method of Haeberli & Hoelzle (1995) described in the methods section.

The hypsometric distribution (Jiskoot et al. 2009) of the ice-covered area is depicted in Fig. 3A, including the distinction between bare and debris-covered ice. The largest mountain glaciers in the area show large portions of heavily debris-covered ice. Interestingly, these debris-covered portions were not only identified on the flatter, distal parts of the glacier tongues, but also in the upper, steeper glacier portions.

The mean slope of glaciers, as derived from the ALOS PRISM DSM, can be appreciated in Fig. 4A. In general terms, the largest glaciers have gentler slopes and vice versa, since the large mountain glaciers have flatter tongues, whereas the small glaciers, mainly permanent snowfields and ice aprons, often occupy steep flanks and couloirs. Small glaciers exhibit a much greater scatter than large ones, indicating that glaciers with similar sizes can largely differ in thickness and glacier volume (Paul & Svoboda 2009). Also noteworthy is the fact that glaciers with northern aspect show less altitudinal scatter than those with southern orientation, meaning that mean elevation is more strongly related to the incoming solar radiation rather than topography (Fig. 4B).

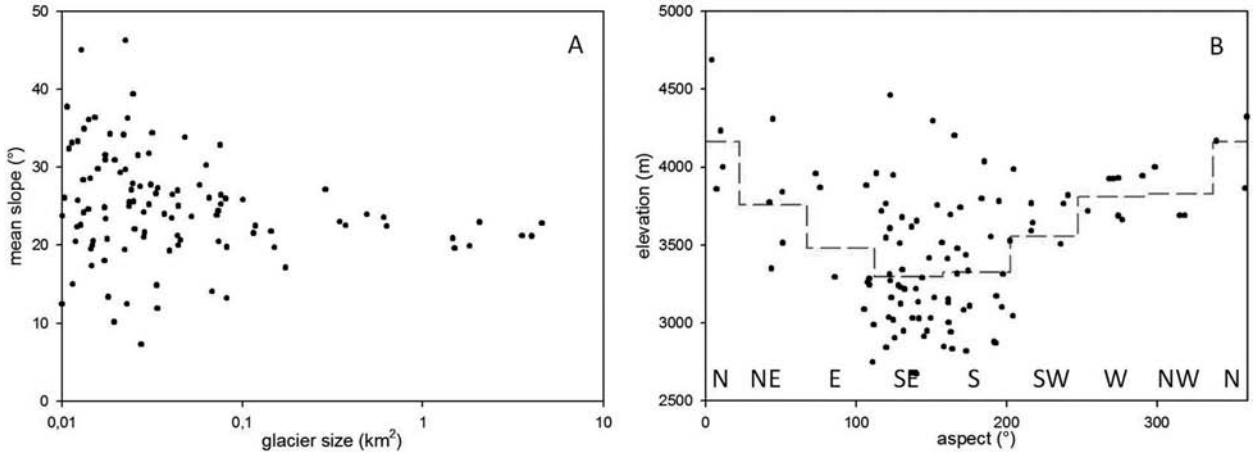

Fig. 4. (A) Scatter plot showing the dependency between glacier size and mean slope, and mean elevation as a function of glacier aspect (B). The dashed red line represents the average elevation for each cardinal sector.

A total loss in glacier area of 9.1 km^2 was measured between 1990 and 2009 (shrinking from 34.5 km^2 in 1990 to 25.4 km^2 in 2009). This represents ~26.4% area reduction in 19 years, and 0.48 km^2 or ~1.4% per year. Figure 2B shows the aspect of the glaciated area for 1990 and 2009. Dividing the total glacier area by this rate of evolution of –0.48 km^2 y^{-1} yields a startling expected lifetime of ~53 years for the inventoried glaciers. As expected for the Southern Hemisphere, the less illuminated southeastern slopes concentrate the majority of the ice-covered terrain. Nevertheless, as evidenced in Fig. 2B, which shows the absolute glacier area loss with respect to orientation, glaciers with southeastern aspects have experienced the largest area losses in absolute terms.

A striking feature is the front of the large glacier at the headwater of Covunco creek (Fig. 5). By analyzing additional Landsat images from 1986, 2003 and 2015, we concluded that the front advanced ~160 m between 1986 and 2003, after which it became largely stable, and we were unable to find evidence of any horizontal retreat of the glacier's snout later on. Additionally, preliminary analyses of aerial photographs from 1968 and 1984 indicate that, in addition to the glacier areal reduction, in most cases the largest mountain glaciers have also experienced significant ice mass losses due to significant surface thinning of the debris-covered tongues. In the headwaters of the Chadileo creek, the main glacier has behaved like a stagnant ice tongue, retreating merely ~125 m since 1968 according to the aerial photographs, but showing an important volume loss due to surface thinning (Fig. 6).

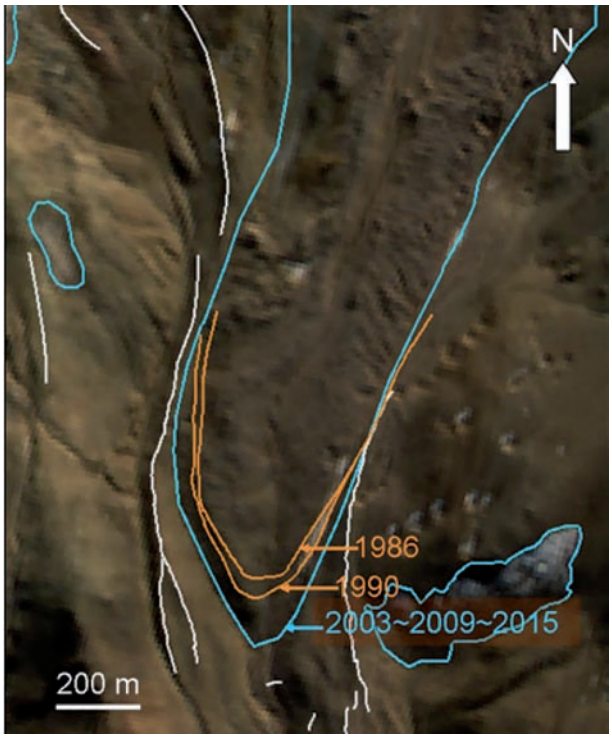

Fig. 5. Frontal position of the glacier located at the head of Covunco Creek. The glacier advanced between 1986 and 2003, and remained stable thereafter. The 2009 extent of the glacier area as mapped in this study is depicted in light blue line, the past frontal positions in orange and moraine crests in white.

Table 1. Rock glacier inventory summary.

Rock glacier activity				
	active	inactive	relict	TOTAL
number	89	84	51	224
area (km^2)	6.4	5	6.3	17.7
mean size (km^2)	0.07	0.06	0.12	–
max size (km^2)	0.71	0.39	0.59	–
max elevation (m)	3968	3526	3340	–
mean elevation (m)	3047	2821	2644	–
min elevation (m)	2664	2165	1955	–

Rock glacier form						
	tongue	lobate	coalescent	spatulate	lobate	TOTAL
number	123	51	78	2	30	224
surface (km^2)	8.2	1	8	0.2	0.3	17.7

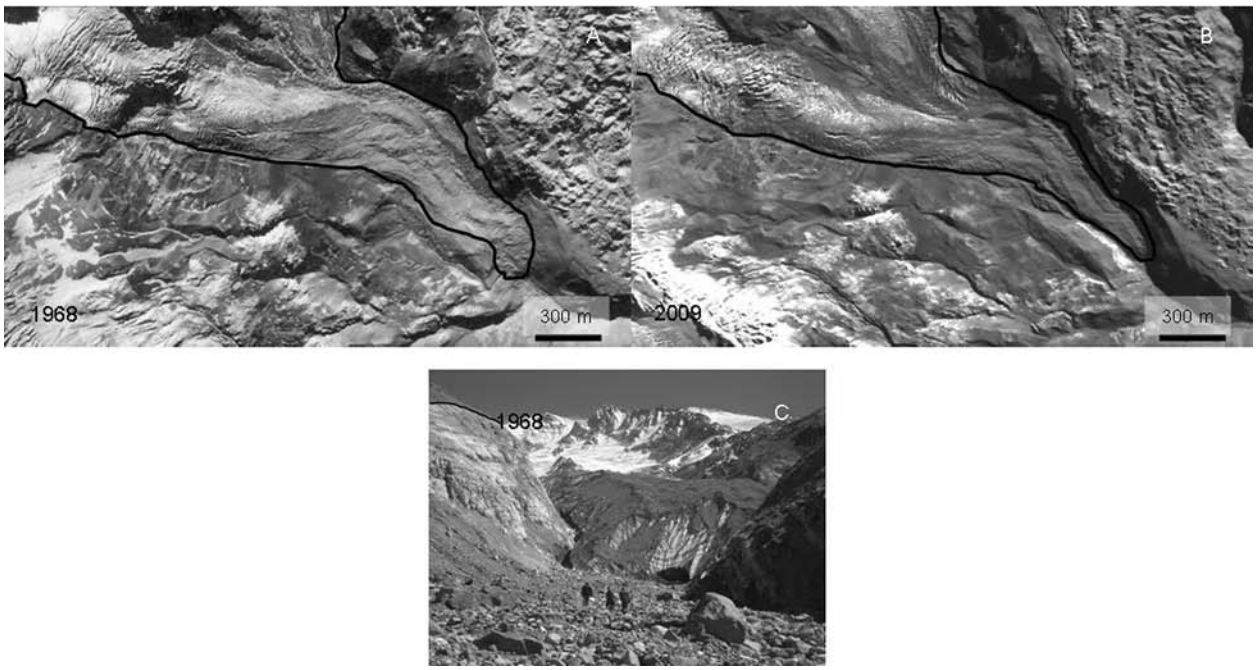

Fig. 6. Outline (black line) for the glacier at the headwater of Chadileo creek and frontal positions for 1968 (aerial photograph, not orthorectified) and 2009 (ALOS PRISM); the volume losses are also in evidence (C): the black line shows the approximate position of the glacier in the 1968 aerial photograph.

4.2. Rock glacier inventory

Intact rock glaciers represent the most abundant landform type, with 173 units (~60% of the inventoried rock glaciers), and a total area of 11.4 km^2, whereas fossil rock glaciers account for 51 landforms and 6.3 km^2. Of the total 173 ice-bearing, intact landforms, 89 (6.4 km^2) correspond to active units, and 84 (5 km^2) to inactive ones, whereas fossil rock glaciers sum up 51 landforms and 6.3 km^2 in area. The rock glacier distribution according to the activity state and form is represented in Table 1.

Rock glaciers are generally simple shaped with a few coalescent units. Polymorphic rock glaciers (*sensu* Frauenfelder & Kääb 2000), where newer lobes successively override older ones, are rare. The largest, non compound rock glacier is located at the headwater of the Covunco creek and has an area of 0.38 km^2. This tongue-shaped landform features (from the proximal to distal portions) areas with debris-free ice patches, debris-covered ice with thermokarst phenomena and hummoky topography, and the rock glacier talus front (Fig. 7). The thermokarst features may be indicative of the melting of dead ice from a former larger glacier, at the top of a creeping ice-debris body, that is, the perennial ice patches can become embedded in the permafrost, may then travel downslope on top of the creeping permafrost and undergo thermokarst processes. At the same time, this landform can be regarded as the southernmost expression of the glacier-rock glacier interaction (Ferri Hidalgo et al. 2015, Monnier & Kinnard 2015). Interestingly, this transition has been not detected in other regions of the Arid and Tropical Andes (Falaschi et al. 2014, Rangecroft et al. 2014).

The majority of the active rock glacier area is located in an altitudinal belt between 2800–3300 m a.s.l. (Fig. 3A), whilst only a few landforms appear at lower elevations in particularly narrow cirques with southern orientation. This responds to the fact that rock glaciers can only occur above the MPL and below the glacier ELA (Haeberli & Burn 2002). On the other hand, rock glacier spatial density results in an average of ~0.9% (Fig. 3B). This is a relatively low value compared to drier Andean areas such as the Andes of Santiago and Mendoza (4%, Azócar & Brenning 2010), or the Valles Calchaquíes district (2.2%, Falaschi et al. 2014).

4.3. Mapping error

By buffering the area of the debris-free glaciers by one pixel and calculating the corresponding relative glacier areal change (Paul et al. 2013), we estimated a mapping error of ca.32% for small glaciers (<1 km^2) and 7% for larger glaciers in the Landsat scene and ca. 12% and 2.5% for the ALOS AVNIR2, respectively.

With respect to rock glaciers, outlines in the ASTER scenes were in average 36% larger than the mean reference areas from the PRISM scenes, whereas the

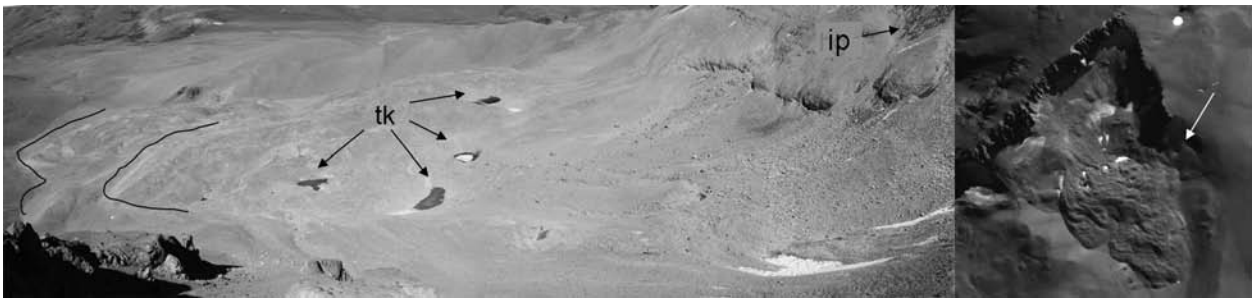

Fig. 7. View of the unique landform containing glacier and rock glacier-type features. Rock glacier fronts are marked with black lines; tk: thermokarst; ip: perennial ice patch. On the right the landform is shown on the PRISM image with the white arrow indicating the point of view of the photo on the left.

variability between analysts in rock glacier size was 56%. Individually, in landforms of small areas (<0.1 km^2), the differences reached errors as high as 400%. From ten digitized rock glaciers, three of them had differences higher than 100%. The rock glaciers outlines digitized from the AVNIR2 images resulted in smaller areas with respect to PRISM by only 4%, and no outlines had individual differences higher than 100%. The superficial structure with furrows and ridges begins to be recognizable in the AVNIR2 10 m resolution scene, though there is still considerable difficulty in mapping the subdued inactive and fossil landforms at this resolution.

By applying the approach of Paul et al. (2013) for rock glaciers (instead of glaciers), the mapping error as obtained with this buffering procedure on the ALOS PRISM images was compared with respect to the on screen digitizing variability. Errors reached maxima of 15%, 21% and 68% for individual polygons smaller than 0.1 km^2, for the 1, 2 and 3 pixel buffers respectively, whereas differences of up to 3%, 5% and 13% (1, 2, 3 pixel buffers) were found for rock glaciers larger than 0.1 km^2. Since the mapping variability from the multiple digitalization round had a maximum value of 38%, and for this study in particular, the mapping error could be located between 2–3 pixels.

5. Discussion

5.1. Glacier changes and climate records

In the Volcán Domuyo area, although ablation areas in the larger mountain glaciers have experienced the major ice area reduction, it was also noticeable progressively larger internal rock outcrops in the accumulation areas as well, which may be indicative of a rising ELA. Nonetheless, Pelto (2006) suggested that significant glacier thinning over the entire surface (including both the accumulation and ablation zones) is in fact indicative of a glacier in disequilibrium state. Thus, a glacier will not be able to reach an equilibrium state, now matter how large the extent of glacier retreat is.

As noted above, both debris-covered and debris-free ice occupy, to a large extent, a similar altitudinal range. This is a common feature of the drier Central Andes, but differs from the moister, southern Patagonian Andes, where debris normally concentrates in the flatter portions of the glaciers (Falaschi et al. 2013, Masiokas et al. 2015). The strong winds, large thermal amplitude, and a high percentage of clear days that are found in the Central Andes are responsible for intensifying cryogenic processes and frost weathering. Due to such an abundant debris cover on the glaciers, produced on the glacier from such rock outcrops and surrounding rockwalls, it was simply not possible to derive convincing transient snow lines based on the analysis of satellite imagery.

A theoretical ELA at ~3300 m a.s.l., taken from Condom et al. (2007), would suggest that glaciers in the Volcán Domuyo have low Accumulation Area Ratios (AAR<0.5), which is indicative of glaciers in disequilibrium state and with negative mass balance (Bakke & Nesje 2011). For glaciers in steady-state conditions, mean elevation (calculated as max. elevation + min. elevation divided by 2) is a rather robust approximation of the ELA. This way, half the change in minimum altitude over the study period represents a measure of the change in glacier ELA for the corresponding jump from one steady state to the next one. For a subset of mountain glaciers, comprising those with elevation ranges that span the theoretical ELA of 3300 m of Condom et al. (2007), we calculated an average increase of ~17 m in the ELA for the 1990–2009 period. Although this approach is most probably not fully adequate to the present case-study, where ongoing glacier retreat is taking place, it nevertheless provides evidence for a rising ELA in the Volcán Domuyo region.

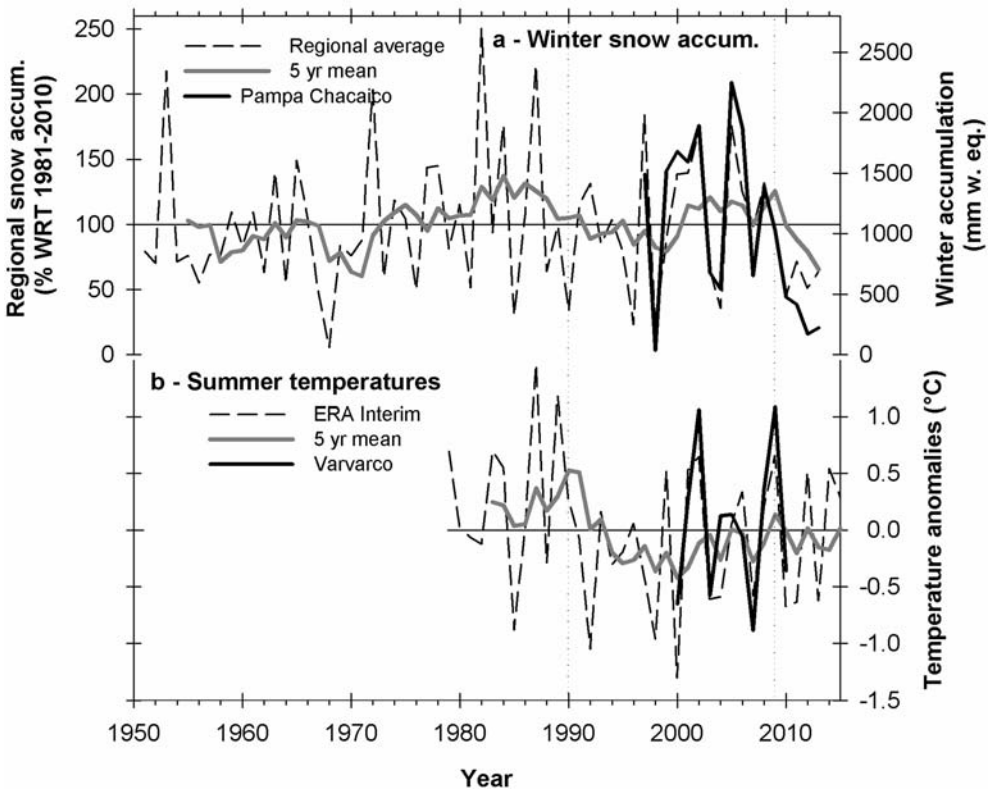

Fig. 8. (a) Winter snowfall (JJA) recorded at the Pampa de Chacaico meteorological station (black line, for location see Fig. 1) compared to a regional snowpack series (dashed black line) developed for the Central Andes by Masiokas et al. (2012). The local record is expressed in mm. of water equivalent whereas the regional values are expressed as percentages from their 1981–2010 mean. A 5-yr moving mean is also plotted (grey line) to emphasize intra-decadal variations in this regional series. (b) Warm season (DJF) mean temperatures as recorded at the Varvarco station (black line, see Fig. 1) compared to those of the 700 mb geopotential height ERA Interim values corresponding to the grid cell centered at 36.5° S–70.25° W (dashed black line). A 5-yr moving mean was also plotted (grey line) to emphasize lower frequency variations in the reanalysis series. The years 1990 and 2009 are shown with dashed lines.

Present-day MAAT for an ELA located at 3300 m was calculated from the temperature records of Pampa de Chacaico weather station (36°28' S – 70°36' W, 2580 m, Fig. 1), yielding a value of ca. –0.4 °C. Furthermore, the ELA lies relatively close to the MPL, or at least is far from being inside the continuous permafrost area, which would in turn be located above 4500 m if the –8 °C isotherm is used as approximation (Haeberli & Burn 2002). Consequently, the above would point out to temperate to polythermal glaciers in a transitional maritime to continental climate setting.

As explained earlier on, glaciers in the Andes between 36° S and 45° S are restricted to the tops of ice-capped volcanoes, mostly in Chilean territory. Since many of these volcanoes have been notably active in recent historic times, it has accordingly been the volcanic activity and not climate factors the main responsible for glacier recession (Rivera & Bown 2013). This is the case of the Nevados de Chillán volcanic complex (36°52' S, 71°22' W – the nearest glaciers to the Volcán Domuyo), where Rivera & Bown (2013) estimated a glacier area loss rate of –0.36 km^2 per year for the 1975–2011 period. Although the cooling of a magmatic chamber in depth of Volcán Domuyo generates important geothermic activity, the heat flux should not be comparable to that of a volcanic eruption (Eduardo Llambías 2013, personal communication). Hence, the larger glacier area loss rate of –0.48 km^2 y^{-1} of the Volcán Domuyo may be related to other factors.

Figure 8a shows the maximum winter snow accumulation values (expressed as mm of snow water equivalent, SWE) between 1997 and 2013 for the Pampa de Chacaico station. This station contains the longest reliable snowpack record in the area (1997–2013), which is

strongly positively correlated (r = 0.89) with a regional winter snowpack series derived from eight selected stations from the Central Andes (30°–37° S; Masiokas et al. 2012). Given this strong positive association, we used the longer regional snowpack series to infer past changes in winter accumulation at the Domuyo glaciers. Over the 1951–2013 period this regional series shows a high interannual variability with an alternation of dry and humid periods but no clear long term trend. However, and in particular after the year 2005, the regional series shows a tendency towards substantially drier conditions that is also evident in the Pampa de Chacaico record. Overall dry conditions were also observed in the early 1990s (Fig. 8a). Garreaud et al. (2013) also found a recent diminishing trend in precipitation (of about 200 mm per decade) for this region, and associated this related with debilitating westerlies over the northern Patagonian Andes.

In the case of temperature records, the excellent correspondence between the Varvarco and ERA Interim reanalysis (700 mb geopotential height) temperature series is shown in Figure 8b. The graph reveals that, after an apparently warm interval in the late 1980s, temperatures dropped in the 1990s but showed a slight increase in the early 21st century.

5.2. Mountain Permafrost lower limit

The pioneer works of Haeberli (1985) and more recently Brenning (2005) indicated that in certain mountain areas, the elevation of the lowermost active rock glacier fronts is indicative of the lower limit of the discontinuous mountain permafrost. Hence, and according to this approach, discontinuous mountain permafrost can exist above 2800 m a.s.l. in the Volcán Domuyo region, where the present-day MAAT was estimated in ~2.9 °C using temperature records from the Pampa de Chacaico weather station. This seems consistent with findings at the nearby Volcán Tromen (4100 m, 37°8'S), where we found a few intact rock glaciers at 3000 m. North of the study area, in the Volcán Peteroa region (35°15'S), the lower limit of discontinuous mountain permafrost was located between 2900–3000 m based on similar rock glacier observations, and a mean annual temperature of 1.05 °C was estimated at 3000 m elevation (Trombotto Liaudat et al. 2014, and Dario Trombotto 2015, personal communication).

On the other hand, we valued an offset in elevation of ~500 m between the estimated ELA and MPL in the Volcán Domuyo region. This offset appears to be a function of latitude (and accordingly, continentality) along the Andes. In the wet, southern Patagonian Andes (47° S), Falaschi et al. (2015) suggested that glaciers and rock glaciers occupy a not overly dissimilar altitudinal range. In the Cordón del Plata range (33° S – Central Andes of Mendoza) the lowermost rock glacier front lie slightly above 3000 m – and the ELA is located at 4150 m (Ruiz & Trombotto Liaudat 2012), whereas for rock glaciers in the Valles Calchaquíes district, (25° S – Cordillera Oriental of Salta), at least 1600 m may separate the theoretic ELA and MPL (Falaschi et al. 2014). Hence, because intact rock glaciers as creeping permafrost features can only exist between the ELA and the MPL, the altitudinal separation between them will also influence the relative abundance of glaciers and rock glaciers in a given region.

In the Central Andes, several previous studies have found rock glaciers under present-day positive MAAT (e.g. Schrott 1996, Trombotto et al. 1997, Brenning 2005). This is contrary to the findings of Haeberli (1983) and Haeberli & Burn (2002), who found that in the Swiss Alps, mean annual air temperatures of –1° C to –2° C are required for occurrence of active rock glaciers. In the Volcán Domuyo area, we calculated an elevation of ~3390 m a.s.l. for the 1997–2013 MAAT –1° C isotherm using mean monthly temperature data from the Pampa de Chacaico station. Nevertheless, permafrost is an entity with slow temperature response rate, which in turn may explain the decadal to century scale survival under surfaces that have warmed to positive temperature conditions (Gruber & Haeberli 2007).

6. Conclusions

In the present study we present the first complete, well documented glacier/rock glacier inventory of the Volcán Domuyo region in the southernmost Central Andes of Argentina. Since a federal law in Argentina 2010 protects all glaciers and rock glaciers in the territory, the inventory presented here adds to the basic information necessary for political decision-making about Andean water resources and for further geocriological research avenues in the region.

The Volcán Domuyo area displays relatively fast-receding residual glaciers and highly-active cryodynamics, with past and present periglacial processes strongly affecting the landscape evolution. In a context of overall glacier retreat, the behavior of the Covunco glacier is unusual, and a possible surge episode needs to be further investigated.

The assessment of rock glacier mapping error is a complicated issue, but the results show that the variability of the digitized outlines decreases with higher spatial resolution. This corroborates the importance of using high-resolution optical imagery for properly mapping small-scale periglacial landforms in any mountainous region. Therefore, we propose that the use of optical satellite images with a 2.5–5 m spatial resolution is ideal for the compilation of rock glaciers.

With no direct evidence from boreholes, geophysical or ground temperature logging data for the study area or for this latitude of the Andes whatsoever, the present day permafrost distribution and content can be hardly determined. This type of detailed measurements, combined with techniques such as Interferometric Synthetic Aperture Radar (InSAR) information to derive rock glacier flow, will be necessary to better understand the current state and recent behavior of rock glaciers in the Domuyo area.

The changes observed in winter accumulation and summer temperatures in the Domuyo region are not conclusive and preclude a clear assessment of the climatic causes behind the observed glacier shrinkage between 1990 and 2009. Detailed in situ glaciological and meteorological measurements are obviously needed to elucidate this important issue.

Acknowledgements: This study was funded by Agencia Nacional de Promoción Científica y Técnica (grant PICT 2007–0379) and received the cooperation of the Japan International Cooperation Agency (JICA) project: Developing a glacier inventory in the Argentinean Andes using high resolution ALOS (Advanced Land Observing Satellite) data. The authors would like to thank Wilfried Haeberli for his suggestions for further improving the analyses of the present study. Thanks also to Dario Trombotto, Mariano Castro, Lidia Espizúa and Solange Páez from IANIGLA, Eduardo Llambías (Centro de Estudios Geológicos, La Plata, Argentina) and the Inventario Nacional de Glaciares initiative of Argentina. Finally, thanks to Samuel Nussbaumer (World Glacier Monitoring Service, Zurich), Ana Paula Salcedo, Yanina Rubio and Marcelo Neme from the Dirección Provincial de Recursos Hídricos de Neuquén, Héctor Valdéz, Daniel and Heraldo Castillo (Área Natural Protegida del Sistema Domuyo), who provided field support.

References

Azócar, G. & Brenning, A. (2010): Hydrological and geomorphological significance of rock glaciers in the dry Andes, Chile (27–33 S). – Permafrost and Periglacial Processes 21: 42–53.

Bakke, J. & Nesje, A. (2011): Equilibrium-Line Altitude. – In: Singh, V., Singh, P. & Haritashya, U. (eds.): Encyclopedia of snow, ice and glaciers: 272 pp.; Springer.

Barsch, D. (1996): Rock glaciers. Indicators for the Permafrost and Former Geoecology in High Mountain Environment. – Springer, Berlin, 331 pp.

Benn, D.I. & Evans, D.J.A. (2010): Glaciers and glaciation. 2nd edition. – Hodder Education, London, 816 pp.

Bodin, X., Rojas, F. & Brenning, A. (2010): Status and evolution of the cryosphere in the Andes of Santiago (Chile, 33.5° S.). – Geomorphology 118: 453–464.

Brenning, A. (2005): Geomorphological, Hydrological and Climatic Significance of Rock Glaciers in the Andes of Central Chile (33–35° S). – Permafrost and Periglacial Processes 16: 231–240.

Brenning, A. & Azócar, G.F. (2010): Statistical Analysis of Topographic and Climatic Controls and Multispectral Signatures of Rock Glaciers in the Dry Andes, Chile (278–338S). – Permafrost and Peroglacial Processes 21: 54–66.

Cheng, G. & Dramis, F. (1992): Distribution of Mountain Permafrost and Climate. – Permafrost and Periglacial Processes 3: 83–91.

Condom, T., Coudrain, A., Sicart, J.E. & Théry, S. (2007): Computation of the space and time evolution of equilibrium-line altitudes on Andean glaciers (10° N–55° S). – Global and Planetary Change 59: 189–202.

De Angelis, H. (2014): Hypsometry and sensitivity of the mass balance to changes in equilibrium line altitude: the case of the South Patagonian Icefield. – Journal of Glaciology 219 (60): 14–28.

Dee, D.P. & 35 co-authors (2011): The ERA-Interim reanalysis: configuration and performance of the data assimilation system. – Quarterly Journal of the Royal Meteorological Society 137: 553–597.

Digregorio, J.H. (1972): Neuquén. – In: Leanza, A.F. (ed.): Geología Regional Argentina. 439–505; Academia Nacional de Ciencias Córdoba.

Digregorio, J.H. & Uliana, M.A. (1980): Cuenca Neuquina. – In: Turner, J.C.M. (ed.): Geología Regional Argentina, Segundo Simposio II: 985–1032; Academia Nacional de Ciencias.

Esper Angillieri, Y. (2009): A preliminary inventory of rock glaciers at 30° S latitude, Cordillera Frontal of San Juan, Argentina. – Quaternary International 195: 151–157.

Falaschi, D., Bravo, C., Masiokas, M., Villalba, R. & Rivera, A. (2013): First Glacier Inventory and Recent Changes in Glacier Area in the Monte San Lorenzo Region (47° S), Southern Patagonian Andes, South America. – Arctic, Antarctic, and Alpine Research 45 (1): 19–28.

Falaschi, D., Castro, M., Masiokas, M., Tadono, T. & Ahumada, A.L. (2014): Rock glacier inventory of the Valles Calchaquíes region (~25° S), Salta, Argentina, derived from ALOS Data. – Permafrost and Periglacial Processes 25 (1): 69–75.

Falaschi, D., Tadono, T. & Masiokas, M. (2015): Rock glaciers in the Patagonian Andes: An inventory for the Monte San Lorenzo (Cerro Cochrane) massif, 47° S. – Geografiska Annaler, Series A, Physical Geography 97 (4): 769–777.

Ferri Hidalgo, L., Zalazar, L., Castro, M., Pitte, P., Masiokas, M.H., Ruiz, L., Villalba, R., Delgado, S., Gimenez, M. & Gargantini, H. (2015): The Glacier Inventory of the Central Andes of Argentina (31°–35° S). – American Geophysical Union 2015 Fall Meeting, San Francisco, 14–18 December 2015.

Frauenfelder, R. & Kääb, A. (2000): Towards a palaeoclimatic model of rock-glacier formation in the Swiss Alps. – Annals of Glaciology 31: 281–286.

Gardelle, J., Berthier, E., Arnaud, Y. & Kääb, A. (2013): Region-wide glacier mass balances over the Pamir-Karakoram-Himalaya during 1999–2011. – The Cryosphere 7: 1263–1286.

Garreaud, R., López, P., Minvielle, M. & Rojas, M. (2013): Large scale control on the Patagonia climate. – Journal of Climate 26: 215–230.

González Díaz, E.F. & Folguera, A. (2005): Reconocimiento y descripción de avalanchas de rocas prehistóricas en el área neuquina delimitada por los paralelos 37°15' y 37°05' S y los meridianos 70°55' y 71°05' O. – Revista de la Asociación Geológica Argentina 60 (3): 446–460.

González Díaz, E.F. & Folguera, A. (2011): Análisis geomorfológico del tramo Medio e inferior de la cuenca de drenaje del río Curri Leuvú, Neuquén. – Revista de la Asociación Geológica Argentina 68 (1): 17–32.

Groeber, P. (1946): Observaciones geológicas a lo largo del meridiano 70. 1. Hoja Chos Malal. – Revista de la Sociedad Geológica Argentina 1 (3): 177–208.

Gruber, S. & Haeberli, W. (2007): Permafrost in steep bedrock slopes and its temperature-related destabilization following climate change. – Journal of Geophysical Research 112 (F02S18).

Haeberli, W. (1983): Permafrost-glacier relationships in the Swiss Alps – today and in the past. – In: Proceedings of the Fourth International Conference on Permafrost. Fairbanks, Alaska. 415–420; National Academy Press.

Haeberli, W. (1985): Creep of mountain permafrost: internal structure and flow of alpine rock glaciers. Mitteilungen der Versuchsanstalt für Wasserbau, Hydrologie und Glaziologie der ETH Zürich 77. – ETH Zurich, Switzerland, 142 pp.

Haeberli, W. & Burn, C. (2002): Natural hazards in forests – glacier and permafrost effects as related to climate changes. – In: Sidle, R.C. (ed.): Environmental Change and Geomorphic Hazards in Forests: 167–202; IUFRO Research Series.

Haeberli, W. & Hoelzle, M. (1995): Application of inventory data for estimating characteristics of and regional climate-change effects on mountain glaciers: a pilot study with the European Alps. – Annals of Glaciology 21: 206–212.

Ikeda, A. & Matsuoka, N. (2002): Degradation of Talus-derived Rock Glaciers in the Upper Engadin, Swiss Alps. – Permafrost Periglacial Processes 13: 145–161.

Jiskoot, H., Curran, C.M., Tessler, D.L. & Shenton, L.R. (2009): Changes in Clemenceau Icefield and Chaba Group glaciers, Canada, related to hypsometry, tributary detachment, length-slope and area-aspect relations. – Annals of Glaciology 50 (53): 133–143.

Kääb, A. (2007): Rock glaciers and protalus forms. – In: Elias, S. (ed.): Encyclopedia of Quaternary Science, 2236–2242; Elsevier.

Leclerq, P.W., Pitte, P., Giessen, R.H., Masiokas, M.H. & Oerlemans, J. (2012): Modelling and climatic interpretation of the length fluctuations of glaciar Frías (north Patagonian Andes, Argentina) 1639–2009AD. – Climate of the Past 8 (5): 1385–1402.

Llambías, E., Palacios, M., Danferder, J.C. & Brogioni, N. (1978): Petrología de las rocas ígneas cenozoicas del Volcán Domuyo y áreas adyacentes, Provincia del Neuquén. – Actas II, VII Congreso Geológico Argentino, Neuquén, pp. 553–568.

Llambías, E., Palacios, M., Danferder, J.C. & Brogioni, N. (1978b): Las rocas ígneas cenozoicas del Volcán Domuyo y áreas adyacentes. – Actas II, VII Congreso Geológico Argentino, Neuquén, pp. 569–584.

Masiokas, M.H., Delgado, S., Pitte, P., Berthier, E., Villalba, R., Skvarca, P., Ruiz, L., Ukita, J., Yamanokuchi, T., Tadono, T., Marinsek, S., Couvreux, F. & Zalazar, L. (2015): Inventory and recent changes of small glaciers on the northeast margin of the Southern Patagonia Icefield, Argentina. – Journal of Glaciology 61 (227): 511–523.

Masiokas, M.H., Villalba, R., Christie, D.A., Betman, E., Luckman, B.H., Le Qesne, C., Prieto, M.R. & Mauget, S. (2012): Snowpack variations since AD 1150 in the Andes of Chile and Argentina (30°–37° S) inferred from rainfall, tree-ring and documentary records. – Journal of Geophysical Research 117: 1–11.

Mercer, J. (1967): Southern Hemisphere Glacier Atlas. Technical Report 67–76-ES. – American Geographical Society, New York, 325 pp.

Monnier, S. & Kinnard, C. (2015): Reconsidering the glacier to rock glacier transformation problem: New insights from the Central Andes of Chile. – Geomorphology 238: 47–55.

New, M., Lister, D., Hulme, M. & Makin, I. (2000): A high-resolution data set of surface climate over global land areas. – Climate Research 21: 1–25.

Nogami, M. (1972): The snow line and climate during the last glacial period in the Andes mountains. – The Quaternary Research (Japan) 11: 71–80.

Paul, F. & Andreassen, L.M. (2009): A new glacier inventory for the Svartisen region, Norway, from Landsat ETM data: challenges and change assessment. – Journal of Glaciology 55: 607–619.

Paul, F., Barrand, N., Berthier, E., Bolch, T., Casey, K., Frey, H., Joshi, S.P., Konovalov, V., Le Bris, R., Mölg, N., Nosenko, G., Nuth, C., Pope, A., Racoviteanu, A., Rastner, P., Raup, B., Scharrer, B., Steffen, K.S. & Winsvold, S. (2013): On the accuracy of glacier outlines derived from remote sensing data. – Annals of Glaciology 54 (63): 171–182.

Paul, F., Kääb, A. & Haeberli, W. (2003): Mapping of rock glaciers with optical satellite imagery. – In: Haeberli, W. & Brandova, D. (eds.): Extended Abstracts on Current Research and Newly Available Information, 8th International Conference on Permafrost. Zurich: 125–126; ICOP 2003 Permafrost.

Paul, F. & Svoboda, F. (2009): A new glacier inventory on southern Baffin Island, Canada, from ASTER data: II. Data analysis, glacier change and applications. – Annals of Glaciology 50 (53): 22–31.

Pelto, M.S. (2006): The current disequilibrium of North Cascade glaciers. – Hydrological Processes 20 (4): 769–779.

Perucca, L. & Esper Angillieri, Y. (2008): A preliminary inventory of periglacial landforms in the Andes of La Rioja and San Juan, Argentina, at about 28° S. – Quaternary International 190: 171–179.

Racoviteanu, A.E., Paul, F., Raup, B., Khalsa, S.J.S. & Armstrong, R. (2009): Challenges and recommendations in mapping of glacier parameters from space: results of the 2008 Global Land Ice Measurements from Space (GLIMS) workshop, Boulder, Colorado, USA. – Annals of Glaciology 50: 53–69.

Rangecroft, S., Harrison, S., Anderson, K., Magrath, J., Castel, A.P. & Pacheco, P. (2014): A First Rock Glacier Inventory for the Bolivian Andes. – Permafrost and Periglacial Processes 25 (4): 333–343.

Rivera, A. & Bown, F. (2013): Recent glacier variations on active ice capped volcanoes in the Southern Volcanic Zone (37°–46° S), Chilean Andes. – Journal of South American Earth Sciences 45: 345–356.

Rivera, A., Bown, F., Carrión, D. & Zenteno, P. (2012): Glacier responses to recent volcanic activity in Southern Chile. – Environmental Research Letters 7 (014036).

Rolleri, E.O. & Criado Roque, P. (1970): Geología de la Provincia de Mendoza. – 4tas Jornadas Geológicas Argentinas, Actas 2, 1–60.

Ruiz, L. & Trombotto Liaudat, D. (2012): Glaciares de Escombros Fósiles en el Cordón Leleque, Noroeste de Chubut: significado paleoclimático. – Revista de la Asociación Geológica Argentina 69 (3): 418–435.

Sagredo, E.A. & Lowell, T.V. (2012): Climatology of Andean glaciers: A framework to understand glacier response to climate change. – Global and Planetary Change 86–87: 101–109.

Salzmann, N., Huggel, C., Rohrer, M., Silverio, W., Mark, B.G., Burns P. & Portocarrero, C. (2013): Glacier changes and climate trends derived from multiple sources in the data scarce Cordillera Vilcanota region, southern Peruvian Andes. – The Cryosphere 7: 103–118.

Schrott, L. (1996): Some geomorphological-hydrological aspects of rock glaciers in the Andes (San Juan, Argentina). – Zeitschrift für Geomorphologie N.F. Suppl. 104, 161–173.

Svoboda, F. & Paul, F. (2009): A new glacier inventory on southern Baffin Island, Canada, from ASTER data: I. Applied methods, challenges and solutions. – Annals of Glaciology 50 (53): 11–21.

Takaku, J. & Tadono, T. (2009): PRISM On-Orbit Geometric Calibration and DSM Performance. – IEEE Transactions on Geoscience and remote Sensing 47 (12): 4060–4073.

Trombotto, D. & Borzotta, E. (2009): Indicators of present global warming through changes in active layer-thickness, estimation of thermal diffusivity and geomorphological observations in the Morenas Coloradas rockglacier, Central Central Andes of Mendoza, Argentina. – Cold Regions Science and Technology 55: 321–330.

Trombotto, D., Buk E. & Hernández, J. (1997): Monitoring of mountain permafrost in the Central Andes, Cordón del Plata, Mendoza, Argentina: – Permafrost Periglacial Processes 8: 123–129.

Trombotto Liaudat, D., Penas, P. & Aloy, G. (2014): Impact of volcanic processes on the cryospheric system of the Peteroa Volcano, Andes of southern Mendoza, Argentina. – Geomorphology 208: 74–87.

Willis, M.J., Melkonian, A.K., Pritchard, M.E. & Ramage, J.M. (2012): Ice loss rates at the Northern Patagonian Icefield derived using a decade of satellite remote sensing. – Remote Sensing of Environment 117: 184–198.

Manuscript received: December 7, 2015
Revised version accepted: January 26, 2016